FULLERENES
AND ATOMIC CLUSTERS

Effect of Carbon Network Defects on the Electronic Structure of Semiconductor Single-Wall Carbon Nanotubes

P. V. Avramov[1, 2], B. I. Yakobson[2], and G. E. Scuseria[2]

[1] *Kirensky Institute of Physics, Siberian Division, Russian Academy of Sciences,*
Akademgorodok, Krasnoyarsk, 660036 Russia

[2] *Center for Biological and Environmental Nanotechnology, Rice University, Houston, Texas, 77005-1892 USA*

Received September 26, 2003

Abstract—For a single-wall (14, 0) carbon nanotube, the total density of electronic states of the ideal structure and of some possible defect structures is calculated in the framework of the band theory approach using Gaussian-type orbitals and the approximation of the generalized density gradient. It is shown that allowance for defects of the atomic structure of a nanotube makes it possible to adequately describe the existing experimental data on nanotube electronic structure. In the framework of the same approach, the total density of electronic states is calculated for an intermolecular contact of (5, 5) and (10, 0) single-wall carbon nanotubes formed due to the creation of a 5–7 defect. It is shown that the electronic states related to the contact region and the 5–7 defect lie in vicinity of the Fermi level. © *2004 MAIK "Nauka/Interperiodica".*

Atomic and electronic structures of a defect (13, 13) carbon nanotube and of an intermolecular contact between the (21, –2) and (22, –5) carbon nanotubes formed by introducing a 5–7 defect were studied using scanning tunneling microscopy (STM) and scanning tunneling spectroscopy (STS) in [1–3]. In those studies, it was shown that a defect introduced into an ideal atomic network of a (13, 13) metal nanotube generates a number of spectroscopic features located between the first Van Hove singularities [1, 3] and that the energy position and intensity of the new spectroscopic features depend on the distance from the defect for which the scanning tunneling spectrum is measured. In [1, 3], the observed oscillations were interpreted in terms of resonant backscattering of the incident electron plane wave by quasibound electronic states of the defect. Experimental STS spectra of the (21, –2)/(22, –5) intermolecular contact measured in the vicinity of the structural defect have shown that the electronic states of the metallic (22, –5) structure and the semiconductor (21, –2) structure are mixed. The relative weights of the spectral features depend on the position of the measurement point with respect to the contact. It has also been shown that the features caused by the contact decay over a distance of several nanometers. Local variations in the densities of states for single-wall nanotubes were experimentally measured in [2] and qualitatively interpreted as interference between the incident and reflected electron waves. The dispersion law in single-wall nanotubes with defects has been interpreted in terms of quantum interference of electrons scattered by defects [1].

Another type of defects in semiconductor carbon nanotubes caused by adsorption of O_2 and NO_2 molecules by the carbon network of these objects was experimentally studied in [4, 5]. Both chemical agents increased the density of electronic states at the Fermi level and converted semiconductor nanotubes into metal nanotubes. On the basis of nonempirical calculations of the electronic structure [6] of a chemisorbed O_2 molecule, these experimental results have been interpreted in terms of extra charge carriers (holes) at the Fermi level and closing of the band gap in semiconductor *p*-type nanotubes.

In the theoretical study performed in [7], on the basis of calculations of the electronic structure of single-wall semiconductor nanotubes performed within the tight-binding model and the local density functional approximation, it was predicted that a 5–7 defect (a Stone–Wales defect) should also result in closing of the band gap in semiconductor nanotubes.

The tight-binding method was also used to calculate a number of intermolecular contacts between nanotubes [8]. These theoretical results have qualitatively confirmed the experimental observations reported in [3].

Nevertheless, correct interpretation of some experimental data even for nonchiral single-wall nanotubes [9] is still lacking. The simplest example is sample no. 7 investigated in the pioneering work [9], where, in particular, the STM spectra of single-wall nanotubes were measured for the first time. According to [9], this sample (of diameter $d = 1.1$ nm with chiral angle $\varphi = 30°$) was a (14, 0) nanotube, which, according to [10], had to have semiconductor properties. Nevertheless, in the

experiment in [9], this sample had metallic properties. In our opinion, the presence of defects in the structure of the carbon (14, 0) nanotube would provide the most reasonable interpretation of such fundamental differences between theory and experiment.

In order to check this assumption, we calculated the electronic structure of an ideal (14, 0) carbon nanotube and a (14, 0) carbon nanotube with different defects [a Stone–Wales defect, double vacancy in the carbon network (2V defect), a defect produced by embedding two additional carbon atoms into the carbon network (an *ad dimmer* defect), and two defects produced by saturating one of the double carbon bonds by the OH and H groups (2OH and 2H defects)]. All calculations were performed using the approximation of a generalized density gradient (the Perdew–Burke–Ernzerhof (PBE) potential) [11] and the band theory approach using Gaussian-type orbitals in the 3–21G, 6–31G, and 6–31G* bases [12]. To correctly describe the electronic structure of isolated defects, the length of the unit cell was taken to be 20 Å. When modeling the variation in the defect density in the atomic network, the length of the unit cell (and, accordingly, the number of carbon atoms in it) was varied. To study the electronic structure of an intermolecular contact, we chose the structure formed by the contact of a metal (5, 5) and semiconductor (10, 0) nanotubes. The intermolecular contact considered is formed by introducing one pentagon and one heptagon into the (5, 5) or (10, 0) nanotube. To model noninteracting contacts, the length of the unit cell was increased to 40 Å.

Optimization of the geometry of defect structures was performed using the method of the analytical gradient of the potential energy surface and the PBE functional [11] in the 3–21G basis. The number of atoms per unit cell was varied from 226 for 2H and 2OH defects (carbon–carbon bonds saturated by two atoms of hydrogen or two functional groups, 2020 functions in the 6–31G basis) to 334 for a 2V defect (3006 functions in the 6–31G basis). The electronic structure of all objects was calculated using 128 points of **k** space in the Brillouin zone. The electronic structure of the ideal (14, 0) nanotube was calculated using both the PBE functional [11] and the hybrid PBE0 functional [13], whose distinctive feature is the admixture of 25% of the exact Hartree–Fock exchange to the pure PBE potential of the density functional theory; this approach makes it possible to take into account electronic correlations in the system more fully. It is believed that this approach [13] is equivalent to the Meller–Plesset fourth-order perturbation theory. The PBE0 functional was shown to provide much better agreement between the total theoretical electronic densities of states (DOS) and the experimental STS spectra of semiconductor nanotubes [14].

The unit cell of the intermolecular (5, 5)/(10, 0) contact contains 360 carbon atoms (3240 functions in the 3–21G basis). The length of the unit cell for this struc-
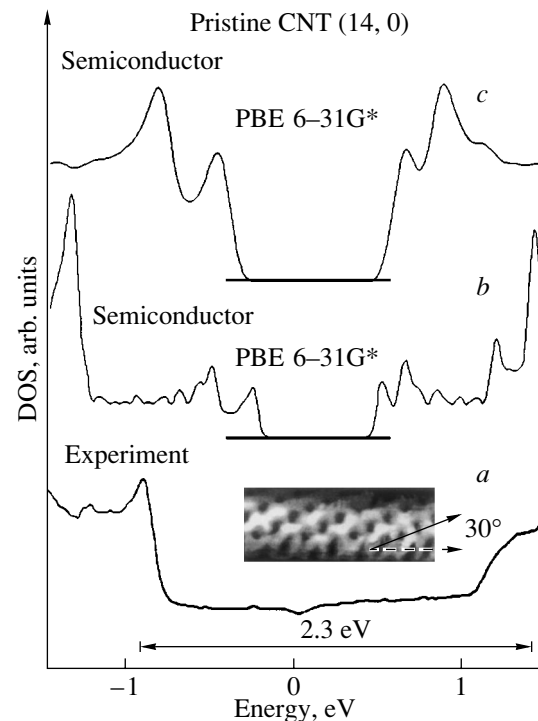

Fig. 1. (*a*) Experimental STS spectra [9] and the theoretical (*b*) PBE and (*c*) PBE0 densities of states (DOS) for semiconductor zigzag (14, 0) carbon nanotubes. The inset shows a photograph of the structure obtained with a scanning tunneling microscope [9]. It is clearly seen that the nanotube has a zigzag structure.

ture is 40 Å. Optimization of the geometry was performed using the semiempirical quantum-chemical PM3 method (for a cluster containing three unit cells) and the analytical gradient of the potential energy. To calculate the electronic structure, 64 points were taken in **k** space in the Brillouin zone. For interpretation of the data on the electronic structure of the intermolecular contact, band calculations for ideal (10, 0) and (5, 5) nanotubes were performed using the PBE potential and 128 points in **k** space.

Figure 1 shows the experimental STS spectra (Fig. 1, *a* [9]) and the theoretical densities of electronic states calculated using the PBE (Fig. 1b) and PBE0 (Fig. 1, *c*) potentials for the ideal semiconductor (14, 0) nanotube. It is seen from Fig. 1 that the experimental spectra exhibit metallic conductivity, which is in disagreement with the previous theoretical prediction [10]. In contrast to the experimental spectrum, the theoretical densities of states obtained using both the PBE and PBE0 potentials agree with the results from [10] and are characterized by the presence of a band gap with a width of about 1 eV (Fig. 1).

Figure 2 shows the experimental spectrum [9] (Fig. 2, *a*) and a set of theoretical spectra for the structures with a Stone–Wales defect (Fig. 2, *b*) and 2H (Fig. 2, *c*), 2OH (Fig. 2d), *ad dimmer* (Fig. 2, *e*), and 2V
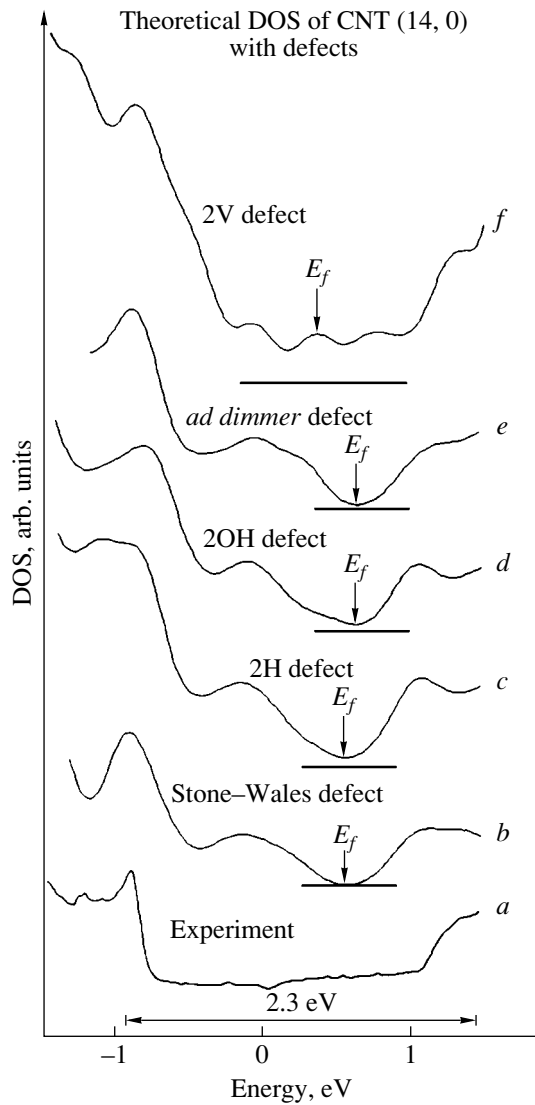
Fig. 2. (*a*) Experimental STS spectrum of a (14, 0) carbon nanotube (CNT) [9], (*b*) theoretical PBE 6–31G density of states for a (14, 0) nanotube with a Stone–Wales defect (the unit cell contains 226 carbon atoms), (*c*) theoretical PBE 6–31G densities of states for a (14, 0) nanotube with a 2H defect (the unit cell contains 226 carbon atoms), (*d*) theoretical PBE 6–31G density of states for a (14, 0) nanotube with a 2OH defect (the unit cell contains 226 carbon atoms), (*e*) theoretical PBE 6–31G density of states for a (14, 0) nanotube with an *ad dimmer* defect created by sorption of a C_2 fragment at the carbon wall (the unit cell contains 282 carbon atoms), and (*f*) theoretical density of states T^R obtained for a rigid band of a 2V defect using the total PBE 6–31G densities of states calculated for 2V defect densities of 0.3 and 0.6% per unit cell (the unit cell contains 334 and 332 carbon atoms, respectively).

defects (Fig. 2, *f*). Introducing structural defects into the ideal graphite network results in the appearance of states in the band gap. In all cases, the main features of the experimental densities of states at energies of approximately –0.9 and 1.4 eV are described ade-

quately. There is a gap in the density of states only for the structure with a Stone–Wales defect (Fig. 2, *b*); all other defects produce metallic-type densities of states.

Characteristic energy-dependent oscillations in the density of states were simulated in [15] by using 1D plane waves $\exp(ikx)$, where x is the space coordinate. The incident plane wave can be resonantly reflected from a quasibound defect state with reflection coefficient $|R|^2$ [$R = |R|\exp(-i(kx + \delta))$, where δ is the phase shift]. The corresponding standing wave can be written as $\psi(k, x) = \exp(ikx) + |R|\exp(-i(kx + \delta))$, which corresponds to spatial oscillations in the densities of states $\rho(k, x) = |\psi(k, x)|^2 = 1 + |R|^2 + 2|R|\cos(2kx + \delta)$ [15].

In order to simulate the effect of the defect density on the electronic structure of nanotubes, we performed calculations of the band structure for a 2V defect with two different cells. The first cell contained one defect per unit cell (334 atoms, which corresponds to a defect density of 0.3%), whereas the second cell had two defects (the unit cell was the same; both defects were placed on opposite ends and opposite faces of the unit cell; the defect density was 0.6%). The translation vector for both unit cells was 25 Å.

Using this special choice of the unit cells, we can write $\mathbf{k}^1 x \sim \mathbf{k}^2 x$ ($\mathbf{k}^1$ is the wave vector of the defect state with the former density and $\mathbf{k}^2$ is that for the defect state with the latter density); therefore, we can obtain the energy positions of the density-of-states oscillations for both unit cells.

For systems with low defect densities, we can use the model of independent centers [16] (assuming that defects do not interact with each other) and the models of rigid bands and impurity bands (a rigid band does not depend on the occupation numbers, whereas the nature of an impurity band is fully determined by the type and density of the impurity). Application of these two models means that we can distinguish between the two independent electronic subsystems of the system (naturally, in narrow intervals of defect densities), namely, the subsystem of defect states T^D and the subsystem T^R formed by the other states with occupation numbers x and $(1 - x)$, respectively.
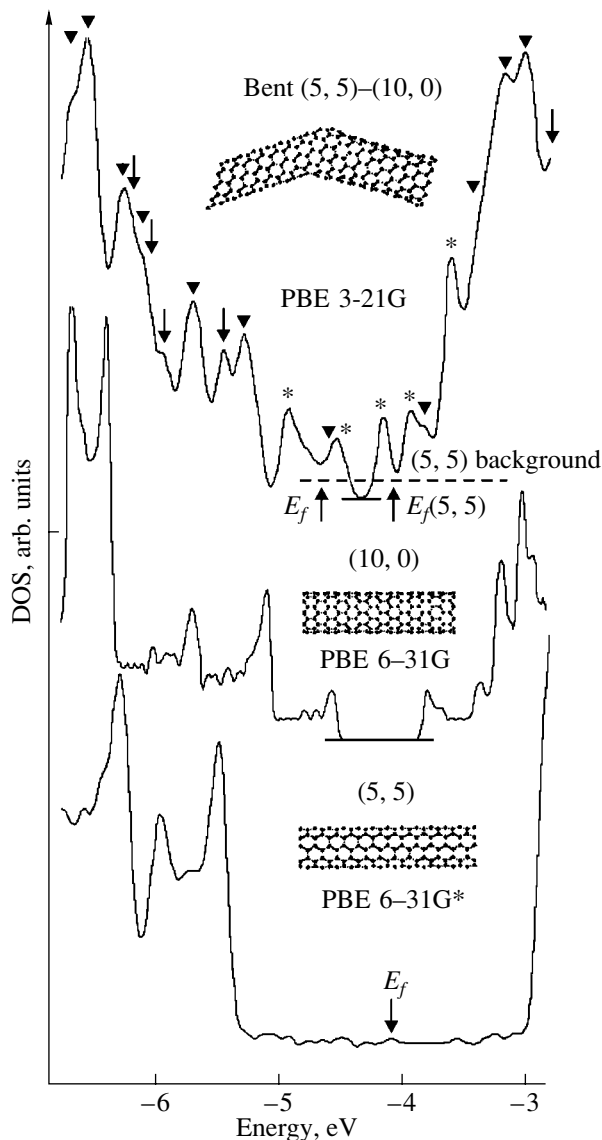
In terms of these two models, we can write two linear equations

$$T_1^T = x_1 T^D + (1 - x_1)T^R,$$
$$T_2^T = x_2 T^D + (1 - x_2)T^R,$$

where T_1^T and T_2^T are the total densities of states for the systems with different defect densities.

For systems with a significant number of noninteracting defects uniformly distributed over the entire atomic network, we can extract the quantity T^R, since different defects can mutually suppress oscillations in the densities of states due to interference effects. Most

Fig. 3. The total densities of states for the (5, 5) and (10, 0) nanotubes and for the (5, 5)/(10, 0) intermolecular contact. Arrows indicate the features related to the (5, 5) structure, triangles indicate the features related to the (10, 0) structure, and asterisks denote the features related to the intermolecular contact itself. The (5, 5), (10, 0), and (5, 5)/(10, 0) structures are shown in the insets.

nanostructures; thus, we may hope for a qualitative description of the electronic structure of the (5, 5)/(10, 0) intermolecular contact (Fig. 3). The length of the unit cell (~40 Å) was chosen to be sufficiently large to avoid significant interaction between the defects. By applying the translational symmetry to the unit cell, we can construct an infinite zigzag structure in which the sections with (5, 5) and (10, 0) structures are separated by the structures containing five- and seven-membered rings (the upper inset in Fig. 3).

Figure 3 shows the densities of states for the (5, 5) and (10, 0) nanotubes and for the (5, 5)/(10, 0) intermolecular contact. According to our nonempirical calculations, the intermolecular contact is metallic with a nonzero density of electronic states at the Fermi level, whose energy position is –4.7 eV. The features near the Fermi level are produced by the electronic states corresponding to the 5–7 defect, whereas the spectral features below and above the Fermi level originate from either (5, 5) or (10, 0) structures.

Comparison of the experimental STS spectra and theoretical electronic densities of states calculated using the band theory approach, Gaussian-type orbitals, and the PBE potential of the approximation of the generalized density gradient shows that the method described above can be successfully applied to calculate the electronic structure of semiconductor single-wall nanotubes with defects. Noticeable differences in the densities of states of ideal nanotubes and nanotubes with defects can serve as an elementary test of the imperfection of the atomic structure of this type of object.

REFERENCES

1. M. Ouyang, J.-L. Huang, and C. M. Lieber, Phys. Rev. Lett. **88**, 066804 (2002).

2. M. Ouyang, J.-L. Huang, C. L. Cheung, and C. M. Lieber, Science **291**, 97 (2001).

3. M. Ouyang, J.-L. Huang, and C. M. Lieber, Annu. Rev. Phys. Chem. **53**, 201 (2002).

4. P. G. Collins, K. Bradley, M. Ishigami, and A. Zettl, Science **287**, 1801 (2000).

5. J. Kong, N. R. Franklin, C. Zhou, M. G. Chapline, S. Peng, K. Cho, and H. Dai, Science **287**, 622 (2000).

6. S.-H. Jhi, S. G. Louie, and M. L. Cohen, Phys. Rev. Lett. **85**, 1710 (2000).

7. V. H. Crespi and M. L. Cohen, Phys. Rev. Lett. **79**, 2093 (1997).

likely, T^R can be seen in spectroscopic experiments for such systems.

Figure 2, f shows T^R obtained by using the theoretical densities of states for unit cells with 2V-defect densities of 0.3 and 0.6%. It is clearly seen that such an approach provides an opportunity to quantitatively describe the experimental density of states obtained in [9] for a (14, 0) nanotube.

The calculations described above show the high quality of the results obtained for defect 1D carbon

8. S. G. Louie, Top. Appl. Phys. **80**, 113 (2001).

9. J. W. G. Wildöer, L. C. Venema, A. G. Rinzler, R. E. Smalley, and C. Dekker, Nature **391**, 59 (1998).

10. J. W. Mintmire, B. I. Dunlop, and C. T. White, Phys. Rev. Lett. **68**, 631 (1992).

11. J. P. Perdew, K. Burke, and M. Ernzerhof, Phys. Rev. Lett. **77**, 3865 (1996); Phys. Rev. Lett. **78**, 1396(E) (1997).

12. M. J. Frisch, G. W. Trucks, H. B. Schlegel, *et al.*, *GAUS-SIAN 01. Development Version* (Gaussian, Pittsburgh, PA, 2001).

13. M. Ernzerhof and G. E. Scuseria, J. Chem. Phys. **110**, 5029 (1999); C. Adamo and V. Barone, J. Chem. Phys. **110**, 6158 (1999).

14. P. V. Avramov, K. N. Kudin, and G. E. Scuseria, Chem. Phys. Lett. **370**, 597 (2003).

15. M. Ouyang, J.-L. Huang, and C. M. Lieber, Annu. Rev. Phys. Chem. **53**, 201 (2002).

16. P. V. Avramov and S. G. Ovchinnikov, Fiz. Tverd. Tela (St. Petersburg) **37**, 2559 (1995) [Phys. Solid State **37**, 1405 (1995)].

Translated by I. Zvyagin